

# Model for the Fluorescence Induction Curve of Photoinhibited Thylakoids

Dmitrii V. Vavilin,<sup>\*,#</sup> Esa Tyystjärvi,<sup>\*</sup> and Eva-Mari Aro<sup>\*</sup>

<sup>\*</sup>Department of Biology, University of Turku, Laboratory of Plant Physiology, BioCity A, FIN-20014 Turku, Finland, and <sup>#</sup>Department of Biophysics, Faculty of Biology, Moscow State University, Moscow 119899, Russia

**ABSTRACT** The fluorescence induction curve of photoinhibited thylakoids measured in the presence of 3-(3,4-dichlorophenyl)-1,1-dimethyl urea was modeled using an extension of the model of Lavergne and Trissl (*Biophys. J.* 68:2474–2492), which takes into account the reversible exciton trapping by photosystem II (PSII) reaction centers and exciton exchange between PSII units. The model of Trissl and Lavergne was modified by assuming that PSII consists of photosynthetically active and photoinhibited (inactive in oxygen evolution) units and that the inactive PSII units can efficiently dissipate energy even if they still retain the capacity for the charge separation reaction. Comparison of theoretical and experimental fluorescence induction curves of thylakoids, which had been subjected to strong light in the presence of the uncoupler nigericin, suggests connectivity between the photoinhibited and active PSII units. The model predicts that photoinhibition lowers the yield of radical pair formation in the remaining active PSII centers. However, the kinetics of PSII inactivation in nigericin-treated thylakoids upon exposure to photoinhibitory light ranging from 185 to 2650  $\mu\text{mol photons m}^{-2} \text{s}^{-1}$  was strictly exponential. This may suggest that photoinhibition occurs independently of the primary electron transfer reactions of PSII or that increased production of harmful substances by photoinhibited PSII units compensates for the protection afforded by the quenching of excitation energy in photoinhibited centers.

## INTRODUCTION

Illumination of chloroplasts causes inactivation of electron transfer through photosystem II (PSII) and subsequent breakdown of the D1 reaction center protein (for recent reviews see Prasil et al., 1992; Aro et al., 1993; Chow, 1994). This type of PSII inactivation is called photoinhibition. High-light induced photoinhibition is accompanied by quenching of maximum ( $F_M$ ) and variable ( $F_V$ ) fluorescence (see Krause and Weis, 1991). The photoinhibitory quenching of fluorescence is most probably caused by increased thermal dissipation of excitation energy in the photochemically inactive (photoinhibited) PSII centers (Powles and Björkman, 1982; Giersch and Krause, 1991; Renger et al., 1995). Such increased thermal dissipation has often been suggested to protect the remaining active PSII centers from photoinhibition (Öquist et al., 1992; Anderson and Aro, 1994; Chow, 1994; Krause, 1994), although the first-order kinetics of photoinhibition lends no support to the idea of protection (Tyystjärvi et al., 1994). One of the purposes of this study was to find a theoretically and experimentally solid basis for estimating the effect of efficient thermal

dissipation in the photoinhibited PSII centers on the primary reactions carried out by the remaining active PSII units.

Efficient energy migration between PSII units manifests itself in the typical sigmoidal shape of the fluorescence induction curve measured in the presence of DCMU. Only so-called PSII<sub>α</sub> units have a capacity for such energy transfer (Melis and Homann, 1976). It has been suggested that the connectivity between active and photoinhibited PSII<sub>α</sub> units is retained, resulting in a quasi-linearity between the  $F_V/F_M$  ratio and proportion of active PSII (Giersch and Krause, 1991).

Lavergne and Trissl (1995; Trissl and Lavergne, 1995) have built a novel model for fluorescence induction taking into account reversible exciton trapping by PSII reaction centers and exciton exchange between PSII units. In the present study we extend this model to photoinhibited thylakoids by assuming that photoinhibited reaction centers do not trap excitons but efficiently dissipate the absorbed light energy in a non-radiative way. Comparison of theoretical and experimental fluorescence induction curves of thylakoids subjected to strong light supports the hypothesis of connectivity between the photoinhibited and active PSII units.

For the case of continuous strong illumination our model predicts that photoinhibition causes a decrease in the efficiency of primary charge separation in the remaining active PSII. Analysis of kinetics of PSII inactivation revealed, however, no evidence for the protective role of the photoinhibited PSII centers. This apparent contradiction might be extricated by suggesting (1) that primary photosynthetic reactions do not play a major role in the mechanism of PSII photoinhibition in thylakoids, or (2) that the primary electron transfer reactions still occurring in some of the photoinhibited PSII centers induce inhibition of the remaining

Received for publication 21 July 1997 and in final form 9 April 1998.

Address reprint requests to Eva-Mari Aro, Department of Biology, University of Turku, Laboratory of Plant Physiology, BioCity A, FIN-20014 Turku, Finland. Tel.: 358-2-3335931; Fax: 358-2-333-8075; E-mail: evaaro@utu.fi.

**Abbreviations used:** BQ, parabenzoquinone; Chl, chlorophyll; DCMU, 3-(3,4-dichlorophenyl)-1,1-dimethyl urea; PFD, photon flux density; Pheo, primary pheophytin  $\alpha$  electron acceptor in photosystem II; PSI and PSII, photosystems I and II; P680, primary chlorophyll  $\alpha$  electron donor in Photosystem II; Q<sub>A</sub> and Q<sub>B</sub>, primary and secondary quinone electron acceptors in photosystem II; qE, energy-dependent component of non-photochemical fluorescence quenching; Tyr<sub>Z</sub>, electron donor to P680.

© 1998 by the Biophysical Society

0006-3495/98/07/503/10 \$2.00

active centers, and the efficiency of the inhibitory process matches the protection afforded by the same centers.

## MATERIALS AND METHODS

Pea (*Pisum sativum* L.) plants were grown in 16 h light/8 h dark rhythm in a phytotron under the relative humidity of 70% and temperature 20°C. The photon flux density during the light phase was 350  $\mu\text{mol photons m}^{-2} \text{s}^{-1}$ . Routinely, the leaves of 3- to 4-week-old plants were harvested at the end of the dark period and then cooled for 1–2 h in darkness at 2°C before thylakoid isolation. Light-adapted leaf material was, however, used in experiments in which D1 protein degradation was measured.

Thylakoids were isolated as described earlier (Tyystjärvi, 1993) and finally suspended in a medium containing 0.3 M sorbitol, 40 mM Hepes-KOH (pH 7.6), 10 mM KCl, 10 mM NaCl, 5 mM  $\text{MgCl}_2$ , 1 mM  $\text{KH}_2\text{PO}_4$ , and 0.1% BSA. The uncoupler nigericin (1  $\mu\text{M}$ ) was included in the medium to prevent the light-induced formation of pH gradient across the thylakoid membrane and development of energy-dependent excitation quenching (qE). Isolated thylakoids were stored in darkness on ice and used for the experiments within 4 h after preparation.

The photoinhibitory treatment was then performed by exposing 20–25 ml of the thylakoid suspension (20  $\mu\text{g Chl ml}^{-1}$ ) to white light from a slide projector. During the treatment the thylakoid suspension was kept in a 5-cm circular dish at controlled temperature (+1 or 18°C) and continuously stirred with a magnetic bar.

Oxygen evolution was measured at 25°C with a Hansatech oxygen electrode (Hansatech, King's Lynn, UK). Continuous light was provided by a KL 1500 illuminator (Walz, Effeltrich, Germany) through two fiber-optic bundles positioned on opposite sides of the  $\text{O}_2$  measuring chamber that contained the thylakoid samples diluted to 5  $\mu\text{g Chl ml}^{-1}$  in the medium described above (without BSA) and 0.2 mM BQ as an electron acceptor. Under saturating light the thylakoid preparations evolved oxygen at typical rates of  $310 \pm 20 \mu\text{mol O}_2/(\text{mg Chl h})$ .

To characterize the amount of functional PSII centers, 310  $\mu\text{l}$  of the thylakoid suspension concentrated to 100  $\mu\text{g Chl ml}^{-1}$  was illuminated in the presence of 0.4 mM BQ in the oxygen electrode cuvette with a FX-200 flash lamp (EG&G Optoelectronics, Salem, MA) operated at a frequency of 10 Hz and flash energy 1.44 J/flash. A plexiglass rod was used to guide the flashlamp light to the thylakoid suspension from the top. The thylakoid suspension layer was  $\sim 2$  mm thick. By performing the same measurement at lower flash energy, it was assured that the intensity of flashes was high enough to saturate PSII electron transfer in the thylakoid sample.

Fluorescence induction of thylakoids was measured using a Walz PAM 101 fluorometer (Walz, Effeltrich, Germany). Thylakoid suspension (20  $\mu\text{g Chl ml}^{-1}$ ) was placed in a 0.4 ml Walz cuvette, incubated for 3 min in darkness in the presence of 10  $\mu\text{M}$  DCMU, and then illuminated for 3 s with actinic light emitted by PAM 102 L LED lamp (light intensity 20  $\mu\text{mol photons m}^{-2} \text{s}^{-1}$ ). FIP fluorescence software, and ADC-12 card (Q<sub>A</sub>-Data, Turku, Finland) were used to drive the fluorometer and to analyze the results. Decomposition of the fluorescence induction curves into exponential and non-exponential components was done as described in Lavergne and Trissl (1995).

Separation of the polypeptides by SDS-PAGE, immunodetection, and quantification of the D1 protein were performed essentially as in Rintamäki et al. (1994). Light intensity was measured with a Licor Quantum Photometer LI-185B (Li-Cor, Lincoln, NE). Chl concentration was determined in 80% acetone extract according to Porra et al. (1989).

## RESULTS

### Oxygen evolution measurements

Typical changes in the light-saturated rate of  $\text{O}_2$  evolution in thylakoids subjected to photoinhibitory light in the presence of the uncoupler nigericin are shown in Fig. 1. Under all the photoinhibitory light intensities the kinetics of PSII

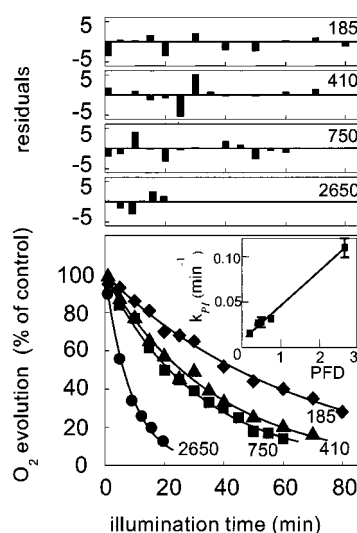


FIGURE 1 Inhibition of PSII oxygen evolution during illumination of thylakoids with 2650 (●), 750 (■), 410 (▲), and 185 (◆)  $\mu\text{mol photons m}^{-2} \text{s}^{-1}$  at 18°C. The residuals indicate the difference between the experimentally measured values and the corresponding values predicted from the best fit to a first-order equation. Oxygen evolution was measured with a continuous saturating light in the presence of 0.2 mM BQ. Incubation of thylakoids in darkness for 80 min caused a 10% decrease in their oxygen-evolving capacity. The inset shows the relationship between the calculated rate constant of photoinhibition ( $k_{PI}$ ) and the photoinhibitory light intensity (PFD) expressed in  $\text{mmol photons m}^{-2} \text{s}^{-1}$ . The bars indicate SD and they are drawn if larger than the symbols.

inactivation was nearly single-exponential and the calculated rate constants for photoinhibition,  $k_{PI}$ , were directly proportional to the photoinhibitory light intensities (see inset to Fig. 1). This is in agreement with previously published results obtained with different PSII preparations (Tyystjärvi et al., 1994) and with intact leaves (Tyystjärvi and Aro, 1996) photoinhibited in the absence of uncoupler. Some deviation from a single-exponential decrease in PSII activity was observed only at light intensity of 2650  $\mu\text{mol photons m}^{-2} \text{s}^{-1}$  after prolonged illumination, when  $>80\%$  of PSII centers were inactivated. Fig. 2 shows that the decrease in the light-saturated rate of  $\text{O}_2$  evolution measured under continuous illumination is almost directly proportional to the decrease in the rate of  $\text{O}_2$  evolution measured using a train of saturating single-turnover flashes. The rate of the flash-induced  $\text{O}_2$  evolution is a direct measure of the concentration of the functional PSII centers. Using isolated PSII particles, Satoh and co-authors (1995) have shown that BQ has a low affinity to the  $\text{Q}_B$ -binding site and hence it accepts electrons predominantly through the plastoquinone pool. Considering that only  $\text{Q}_B$ -reducing centers can donate electrons to the plastoquinone pool, and that the majority of  $\text{Q}_B$ -reducing centers are of PSII <sub>$\alpha$</sub>  type (Guenther et al., 1990), the photoinhibitory decrease in BQ-dependent  $\text{O}_2$  evolution observed in pea thylakoids reflects mainly the kinetics of inactivation of the PSII <sub>$\alpha$</sub>  units.

Fig. 3 shows a comparison of the normalized light-response curves of  $\text{O}_2$  production in control and photoinhib-

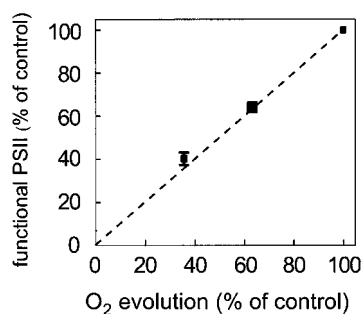


FIGURE 2 Comparison between the inhibition of PSII oxygen evolution (measured with continuous saturating light) and decrease in the concentration of functional PSII in photoinhibited thylakoids (measured as flash-induced oxygen evolution). Thylakoid suspension (20  $\mu\text{g}$  Chl/ml) was subjected to photoinhibitory light of 600  $\mu\text{mol photons m}^{-2} \text{s}^{-1}$  (18°C). Before the photoinhibition treatment and at 30- and 60-min time-points, aliquots were taken from the suspension and diluted to 5  $\mu\text{g}$  Chl/ml or concentrated to 100  $\mu\text{g}$  Chl/ml to measure oxygen evolution under saturating continuous light and to determine the concentration of functional PSII, respectively. The concentration of functional PSII centers in thylakoids was determined by measuring oxygen evolution in response to a 10 Hz train of saturating single-turnover flashes after adding 0.4 mM BQ as an electron acceptor. Each data point represents the mean of three independent experiments. The bars indicate SD and they are drawn if larger than the symbols.

ited thylakoids. Under limiting light, the quantum efficiency of  $\text{O}_2$  evolution normalized to the proportion of active PSII centers was slightly higher in thylakoids photoinhibited for 15 min compared to the non-photoinhibited controls.

### Characterization of the model for fluorescence induction

The model calculations were based on a modification of the procedure described by Lavergne and Trissl (1995). The model assumes a rapid exciton equilibration among all antenna pigments of an individual PSII unit and reversible exciton trapping by open and closed reaction centers (Schatz et al., 1988); exciton exchange between separate

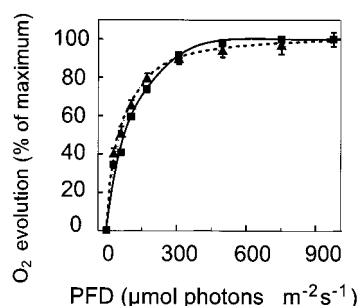


FIGURE 3 Normalized light-response curves of oxygen evolution for control thylakoids (■) and thylakoids photoinhibited for 15 min at 750  $\mu\text{mol photons m}^{-2} \text{s}^{-1}$  at 18°C (▲). Each data point represents the mean of five independent experiments. Bars, drawn if larger than symbols, indicate SD. Oxygen evolution was measured with continuous saturating light. The maximum rates of oxygen evolution were 280 and 150  $\mu\text{mol O}_2/(\text{mg Chl h})$  in control and photoinhibited samples, respectively.

PSII units was described by macroscopic rate constants. The following assumptions were additionally made to describe the primary processes in PSII $_{\alpha}$  in thylakoids pre-subjected to photoinhibitory light.

1. PSII is comprised of photosynthetically active units and units that are inactive in oxygen evolution (photoinhibited) (Giersch and Krause, 1991);
2. Properties of the active PSII units remain unchanged in the course of photoinhibitory treatment;
3. The photoinhibited PSII units efficiently dissipate energy irrespective of their ability to perform the primary charge separation;
4. Photoinhibited and active PSII units have similar antenna size.

A corresponding kinetic model based on the above assumptions is illustrated in Fig. 4. The reactions are characterized by a set of first-order rate constants, namely  $k_{\text{el}}$  for mono-molecular energy losses in antenna ( $k_{\text{el}}$  includes  $k_{\text{fl}}$ , the energy losses by the radiative pathway),  $k_1$  and  $k_{-1}$  for trapping and detrapping excitation energy by the active PSII units,  $k_2$  for charge stabilization, and  $k_d$  for non-radiative energy losses from the radical pair of active PSII. The superscript “INH” is used to indicate the photoinhibited PSII. Superscripts “OX” and “RED” are reserved for active PSII containing oxidized or reduced  $\text{Q}_A$ , respectively. For active PSII we assume that  $k_{\text{el}}^{\text{OX}} = k_{\text{el}}^{\text{RED}} (=k_{\text{el}}^{\text{ACT}})$  and  $k_{\text{fl}}^{\text{OX}} = k_{\text{fl}}^{\text{RED}} (=k_{\text{fl}}^{\text{ACT}})$  (Leibl et al., 1989; Roelofs et al., 1992), where the superscript “ACT” refers to active PSII centers without regard to the reduction state of their  $\text{Q}_A$ .

Calling  $o$  the fraction of open centers,  $r$  the fraction of closed centers, and  $i$  the fraction of photoinhibited centers ( $o + r + i = 1$ ), the macroscopic rate constants for interunit

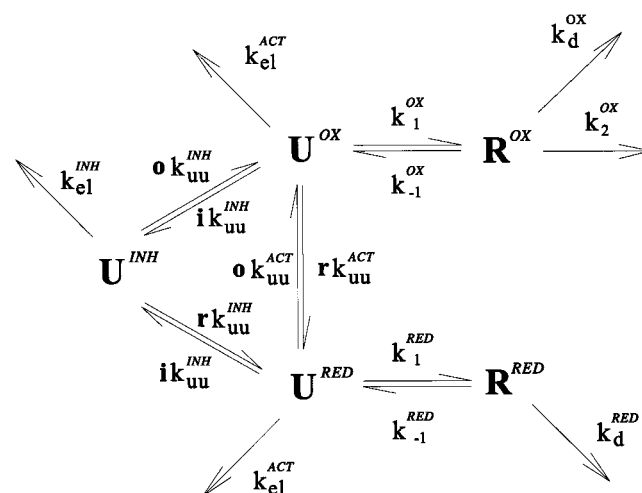


FIGURE 4 Kinetic model for the primary reactions within a system of open, closed, and photoinhibited PSII $_{\alpha}$  units. **R** stands for the radical pair and **U** stands for the antenna system of a PSII unit. Superscripts “OX” and “RED” denote photochemically active PSII units in an open and closed state, respectively. The superscript “INH” denotes the photoinhibited PSII. The rate constants represent processes as described in the text (see also Appendix for the list of symbols).

energy transfer from active PSII units in the open state to active PSII units in the closed state and vice versa are  $rk_{uu}^{ACT}$  and  $ok_{uu}^{ACT}$ , respectively; the rate constants for interunit energy transfer from active PSII units (open state) to photoinhibited units and vice versa are  $ik_{uu}^{INH}$  and  $ok_{uu}^{INH}$ , respectively; and the rate constants for interunit energy transfer from active PSII units (closed state) to photoinhibited units and vice versa are  $ik_{uu}^{INH}$  and  $rk_{uu}^{INH}$ , respectively.

As pointed out (Dau, 1994; Lavergne and Trissl, 1995), the reaction scheme shown in Fig. 4 turns out to be equivalent to a scheme with irreversible trapping processes (Fig. 5) described by a set of *effective* rate constants of energy conversion  $k^{INH}$ ,  $k^{OX}$ , and  $k^{RED}$ . Analytical expressions linking these effective rate constants and the rate constants of the reactions shown in Fig. 4 are listed in the Appendix (Eqs. 1 and 2). The main advantage of the second scheme is that for this case an analytical solution for the fluorescence induction kinetics can be derived and expressed as a function of the rate constants characterizing the inter- and intra-PSII elementary reactions, proportion of the photoinhibited units, and rate of light absorption by individual PSII.

### Analysis of experimental induction curves

The photoinhibitory treatment of thylakoids at  $750 \mu\text{mol photons m}^{-2} \text{s}^{-1}$  caused a significant decline in  $F_M$  and slow rise in  $F_O$ , resulting in a decrease in  $F_V$ . Using a fitting procedure described by Lavergne and Trissl (1995), the measured variable component of the fluorescence induction was decomposed into  $\alpha$  and  $\beta$  contributions by adjusting five parameters (i.e.,  $\Phi_{V\alpha}^{\max}$ ,  $I_\alpha A_\alpha$ ,  $\mathcal{F}_\alpha(1 - i)$ ,  $\Phi_{V\beta}^{\max}$ , and  $I_\beta A_\beta$  see Eqs. 15–17). The result of this analysis shows that the experimental traces of fluorescence induction measured in thylakoids preexposed to strong light for different time periods, and therefore having different proportions of the photoinhibited PSII, can be reasonably well approximated by the theoretical curves composed of sigmoidal ( $\alpha$ ) and exponential ( $\beta$ ) components (Fig. 6, A–D). The parameters

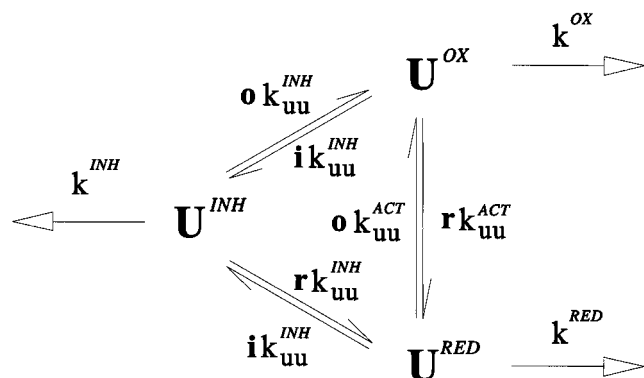


FIGURE 5 Irreversible branched decay scheme equivalent to the exciton radical pair model shown in Fig. 4. The analytical expressions linking the effective rate constants  $k^{INH}$ ,  $k^{OX}$ , and  $k^{RED}$  to the rate constants describing the charge separation reactions depicted in Fig. 4 are listed in the Appendix (Eqs. 1 and 2).

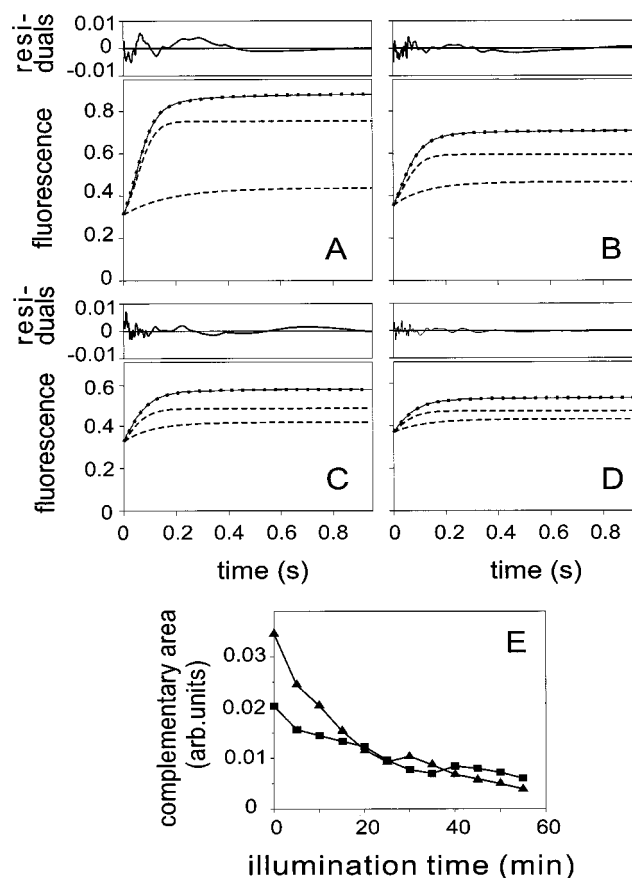


FIGURE 6 (A–D) Examples of experimental fluorescence induction curves (solid lines) and the results of decomposition of the variable part of these curves into nonexponential ( $\alpha$ ) and exponential ( $\beta$ ) components. The dashed lines show the corresponding individual contributions of the  $\alpha$  and  $\beta$  components and the dotted lines indicate the sum of the  $\alpha$  (upper curve) and  $\beta$  (lower curve) components. The residuals show the difference between the experimental curve and the calculated sum of the  $\alpha$  and  $\beta$  components. (E) Effect of light treatment of thylakoids on changes in the complementary area of fluorescence induction calculated for  $\alpha$  ( $\blacktriangle$ ) and  $\beta$  ( $\blacksquare$ ) components. The fluorescence traces were recorded from the thylakoids photoinhibited with  $750 \mu\text{mol photons m}^{-2} \text{s}^{-1}$  at  $18^\circ\text{C}$  for 0 (A), 15 (B), 25 (C), and 45 (D) min (0, 35, 53, and 74% inhibition of light-saturated oxygen evolution, respectively). Five parameters ( $\Phi_{V\alpha}^{\max}$ ,  $\mathcal{F}_\alpha(1 - i)$ ,  $I_\alpha A_\alpha$ ,  $I_\beta A_\beta$ , and  $\Phi_{V\beta}^{\max}$ ) were adjusted to obtain to the best correlation between the experimentally measured curves and those predicted by the theory (Eqs. 15–17). The fitted parameter values were further used for calculation of the complementary areas (E).

obtained were further used to calculate the complementary areas of  $\alpha$  and  $\beta$  contributions. These calculations revealed that both  $\text{PSII}_\alpha$  and  $\text{PSII}_\beta$  centers were gradually inactivated under strong light (Fig. 6 E), but the maximum complementary area of the  $\alpha$  component decreased faster than that of the  $\beta$  component.

One of our objectives was to look for connectivity between the photoinhibited and active  $\text{PSII}_\alpha$  units from the analysis of the shape of the fluorescence induction curves. This can be done by constructing theoretical induction curves from the known values of the rate constants for the primary PSII reactions using Eqs. 8, 15, and 16 (see Ap-



pendix), and comparing them to the experimental traces of fluorescence induction recorded from the photoinhibited thylakoids.

If  $i = 0$  (non-photoinhibited thylakoids), eight rate constants are required to compute  $\Phi_O$  and  $\Phi_M$  yields and  $\Phi_V/\Phi_M$  ratio, whereas additional knowledge on the values for the rate constant for interunit exciton transfer,  $k_{uu}^{ACT}$ , and the rate of exciton creation in PSII units,  $I_\alpha$ , are needed to compute the kinetics of fluorescence rise caused by  $Q_A$  reduction in the PSII $_\alpha$  centers. Following the approach suggested in Lavergne and Trissl (1995; Trissl and Lavergne, 1995) we took the values for the rate constants of primary PSII reactions (except for  $k_{el}^{ACT}$ ) from (Roelofs et al., 1992) and determined the parameter  $k_{el}^{ACT}$  so that the calculated  $\Phi_V/\Phi_M$  ratio agreed with the  $F_V/F_M$  value measured from the non-photoinhibited thylakoids. After a correction for contribution of PSI fluorescence, which has been estimated to comprise  $\sim 25\%$  of  $F_O$  value (Trissl and Lavergne, 1995), the  $k_{el}^{ACT}$  was calculated to be  $(1.65 \text{ ns})^{-1}$ . The values for  $k_{uu}^{ACT}$  and  $I_\alpha$  were set equal to  $(0.25 \text{ ns})^{-1}$  and  $17.5 \text{ s}^{-1}$  to obtain the best correlation between the theoretical and experimental  $\alpha$  components of fluorescence induction (Fig. 7).

When  $i > 0$  (photoinhibited thylakoids), the following additional constants are needed: the rate constant for exciton transfer between the photoinhibited and active PSII units ( $k_{fi}^{INH}$ ), the rate constant for energy losses in the photoinhibited PSII units ( $k_{el}^{INH}$ ), and the rate constant for radiative energy losses in the photoinhibited PSII units ( $k_{fl}^{INH}$ ). We assumed that the rate constant of fluorescence does not change during photoinhibition ( $k_{fl}^{INH} = k_{fl}^{ACT}$ ) and that  $k_{uu}^{INH}$  can take any value between 0 and  $k_{uu}^{ACT}$ . For simplicity, we restricted the treatment to two extreme cases,  $k_{uu}^{INH} = k_{uu}^{ACT}$  and  $k_{uu}^{INH} = 0$ , which corresponds to the case where the photoinhibited centers are fully coupled to the active centers or fully uncoupled from them, respectively.

The value of  $k_{el}^{INH}$  was estimated on the basis of the gradual  $F_O$  increase that accompanied the photoinhibitory treatment of thylakoids. To account for the contribution of the photoinhibited PSII $_\alpha$  to the changes in fluorescence, we assumed that fluorescence yield of PSI is constant during the high-light treatment. Since the complementary area of both PSII $_\alpha$  and PSII $_\beta$  components decreased during photoinhibitory illumination of nigericin-treated thylakoids (see Fig. 6 E), we also assumed for simplicity that PSII $_\alpha$  and PSII $_\beta$  have similar sensitivity to photoinhibition and contribute to gradual rise in  $F_O$  proportionally to their light-harvesting capacity. After these corrections the value of  $k_{el}^{INH}$  was found to be  $\sim (0.46 \text{ ns})^{-1}$ . Fig. 7 A compares theoretical curves and experimental data about  $F_O$  (for PSII $_\alpha$  + PSII $_\beta$ ) and  $F_V$  of PSII $_\alpha$  in different stages of photoinhibition, and Fig. 7, B–E show normalized traces of the  $\alpha$  component of fluorescence induction. The results clearly demonstrate that the model predictions fit the experimental data well if  $k_{uu}^{INH}$  is close to  $k_{uu}^{ACT}$ , suggesting a good connectivity between the photoinhibited and active PSII centers.

Next we tested the effect of photoinhibition on the efficiency of formation of the charge separated state using Eqs.

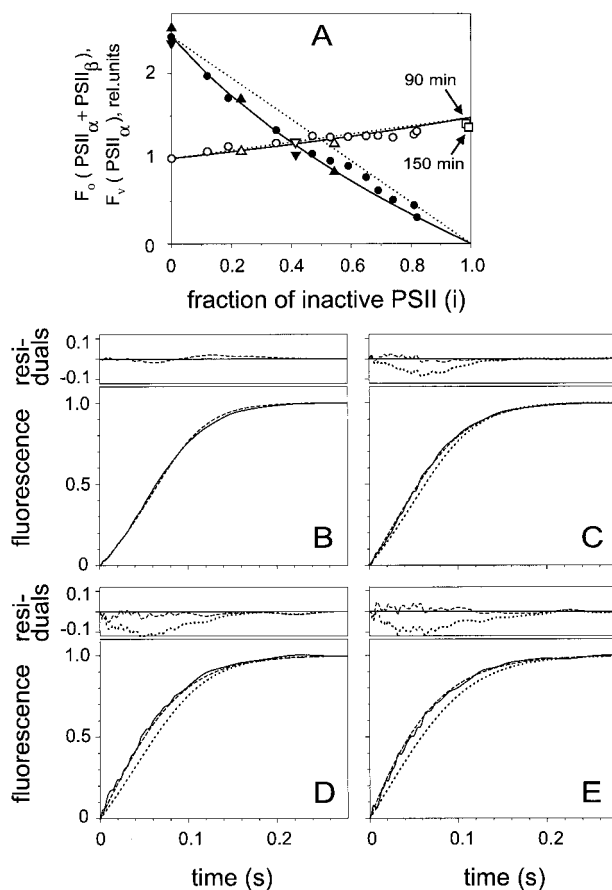


FIGURE 7 Comparison of theoretical predictions based on the model shown in Fig. 4 with experimental data obtained for thylakoids photoinhibited for different periods of time with  $750 \mu\text{mol photons m}^{-2} \text{ s}^{-1}$  at  $18^\circ\text{C}$ . Parameters for  $\alpha$ -centers used for the theoretical calculations:  $k_1^{OX} = (0.33 \text{ ns})^{-1}$ ,  $k_{-1}^{OX} = (3.33 \text{ ns})^{-1}$ ,  $k_d^{OX} = (1000 \text{ ns})^{-1}$ ,  $k_2^{OX} = (0.44 \text{ ns})^{-1}$ ,  $k_1^{RED} = (2.13 \text{ ns})^{-1}$ ,  $k_{-1}^{RED} = (2.94 \text{ ns})^{-1}$ ,  $k_d^{RED} = (1.0 \text{ ns})^{-1}$ ,  $k_{fl} = (18 \text{ ns})^{-1}$  were taken from Roelofs et al. (1993);  $k_{uu}^{ACT} = (0.25 \text{ ns})^{-1}$ ,  $k_{el}^{ACT} = (1.65 \text{ ns})^{-1}$ ,  $k_{fi}^{INH} = (0.46 \text{ ns})^{-1}$ , as calculated in this study. The proportion of photoinhibited PSII centers was estimated by measuring the rate of oxygen evolution in thylakoids with continuous saturating light. (A) Relationship between  $F_O (PSII_\alpha + PSII_\beta)$ ,  $F_V (PSII_\alpha)$ , and proportion of the photoinhibited PSII ( $i$ ). The solid line shows model calculations for  $k_{uu}^{INH} = (0.26 \text{ ns})^{-1}$  and the dotted line shows calculations for  $k_{uu}^{INH} = 0$  with  $i$  taken as a variable. The experimentally measured points for  $F_O$  (open symbols) are shown after subtraction of the constant contribution of PSI fluorescence ( $25\%$  of the experimental  $F_O$ ). Points pointed by arrow indicate the  $F_O$  values measured in thylakoids subjected to the strong illumination for 90 and 150 min, respectively. Closed symbols show values of variable fluorescence  $F_V (PSII_\alpha)$  obtained after decomposition of the recorded fluorescence induction curves into the  $\alpha$  and  $\beta$  components, as described in the legend to Fig. 6. Different types of symbols (i.e., circles, squares, and triangles) are reserved for different independent experiments. (B–E) Normalized traces of fluorescence induction for PSII $_\alpha$  in photoinhibited thylakoids calculated for  $k_{uu}^{INH} = (0.26 \text{ ns})^{-1}$  (dashed line),  $k_{uu}^{INH} = 0$  (dotted line), and derived from the experimentally measured, as described in the legend to Fig. 6 (solid line). The proportion of photoinhibited PSII units  $i$  was 0 (B), 0.32 (C), 0.52 (D), and 0.74 (E). The error residuals are drawn with the same line type as the fitted curve.

20 derived as shown in the Appendix. In this analysis we heeded only the case when all the active PSII centers were in the closed state ( $o = 0$ ) since even the onset of photoin-

hibitory light of lowest intensity used in this study ( $185 \mu\text{mol photons m}^{-2} \text{s}^{-1}$ ) caused closure of almost 100% of the active PSII in isolated thylakoids due to the lack of efficient oxidation of the plastoquinone pool. Fig. 8 displays the relationship between the steady-state concentration of the radical pairs formed under continuous illumination in the active PSII centers ( $R/rI$ ) and the degree of photoinhibition. Normalization to the proportion of the active PSII ( $r = 1 - i$ ) was used to facilitate comparison of the yields obtained at different proportions of inhibited centers. The model calculations clearly demonstrate that the efficiency of the radical pair formation decreases when photoinhibition proceeds.

### D1 protein degradation and changes in the fluorescence yield

When isolated thylakoids were exposed to the photoinhibitory light at  $+1^\circ\text{C}$ , no degradation of the D1 protein took place despite pronounced inactivation of PSII activity evidenced by a lowered  $F_V/F_M$  ratio (Fig. 9). However, if thylakoids that had been inactivated in the cold were transferred to  $18^\circ\text{C}$  in complete darkness, the degradation of the D1 protein proceeded without any further changes in  $F_O$  and  $F_M$  fluorescence yields and PSII activity. Contrary to the experiments described in previous sections, degradation of the D1 protein was measured in thylakoids isolated from light-adapted leaves because, according to our observations (data not shown), the disappearance of the D1 protein in the dark after the low-temperature photoinhibition of thylakoids is retarded if these thylakoids are isolated from dark-adapted leaves.

### DISCUSSION

Photoinhibitory inactivation does not seriously alter the connectivity of PSII $_{\alpha}$ , as evidenced by a good agreement between the modeled and experimentally measured traces of fluorescence induction with the assumption that  $k_{uu}^{\text{INH}} = k_{uu}^{\text{ACT}}$ .

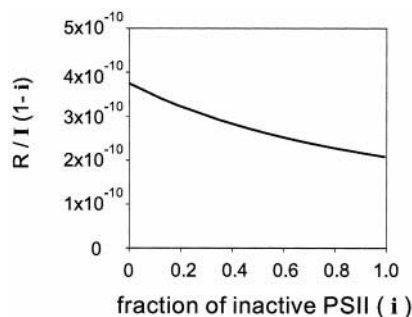


FIGURE 8 The calculated relative efficiency of formation of the charge separated state ( $R/I r$ ) as a function of the proportion of the photoinhibited PSII ( $i$ ). Calculations were done according to Eqs. 20 for  $k_{uu}^{\text{INH}} = (0.26 \text{ ns})^{-1}$ . The other rate constants are as in Fig. 6.

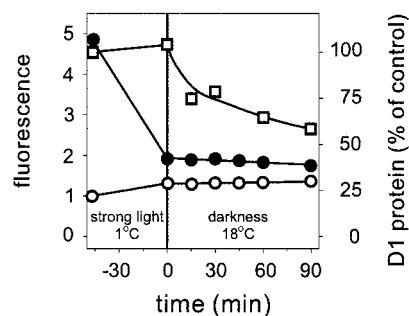


FIGURE 9 Relationship between the D1 protein content ( $\square$ ) and changes in the  $F_O$  ( $\circ$ ) and  $F_M$  ( $\bullet$ ) values in photoinhibited thylakoids. Thylakoids were subjected to photoinhibitory illumination with  $750 \mu\text{mol photons m}^{-2} \text{s}^{-1}$  at  $1^\circ\text{C}$  and then incubated in complete darkness at  $18^\circ\text{C}$ . Time  $t = 0$  indicates the moment when illumination was stopped and the temperature raised up from 1 to  $18^\circ\text{C}$ . The D1 protein content was measured immunologically.

In the mathematical formulation we used, all possible photochemical processes within the photoinhibited PSII were described by a single effective rate constant  $k^{\text{INH}}$ , which was estimated to be of  $\sim(0.46 \text{ ns})^{-1}$  on the basis of  $F_O$  increase during photoinhibition. The value of  $k^{\text{INH}}$  appeared to be noticeably higher than  $k^{\text{RED}}$ , the effective rate constant of exciton decay in the active PSII in the reduced state, that equals  $(1.06 \text{ ns})^{-1}$  according to Eqs. 1c and 2c. This difference in the values of the rate constants is responsible for increased quenching of  $F_M$  in photoinhibited membranes.

As evidenced from Fig. 9, degradation of the D1 protein alters neither  $F_O$  nor  $F_M$  yields in photoinhibited thylakoids. This indicates that the fluorescence quenching associated with photoinhibition is most probably not linked to D1 protein or cofactor molecules bound to it.

Some studies (Styring et al., 1990) have reported that impairment of charge separation is the slowest process of photoinhibition, and therefore the population of photoinhibited PSII complexes, which are unable to evolve oxygen and which have altered fluorescence properties, can be heterogeneous and may consist of PSII units capable and incapable of formation of the radical pair  $\text{P680}^+\text{Pheo}^-$ . It is likely that these two kinds of photoinhibited PSII have similar values of  $k^{\text{INH}}$ , so that there is no need to consider this type of heterogeneity for calculations of the fluorescence yields in photoinhibited thylakoids. The following reasoning might support this statement. As shown in Fig. 7A, nearly 100% loss of  $F_V$  and inactivation of oxygen evolution were observed in thylakoids illuminated for  $\sim 90 \text{ min}$  at  $750 \mu\text{mol photons m}^{-2} \text{s}^{-1}$ . This state was characterized by 25% increase in  $F_O$  yield compared to the nonphotoinhibited control. Styring and co-authors (1990) have shown that the charge separation reaction can remain operational for a considerable amount of time in PSII-enriched membranes with photoinhibited oxygen evolution. In our experiments, the raised  $F_O$  yield undergoes only minor changes if the photoinhibited samples were illuminated for an additional 60 min, a treatment that would undoubtedly destroy charge

separation in most PSII centers and alter  $F_0$  fluorescence if  $k^{\text{INH}}$  is significantly different in photoinhibited PSII with fully operational and impaired charge separation reactions.

By analogy with Eq. 1c, the effective rate constant for energy losses in a hypothetical photoinhibited PSII with functional charge separation  $k^{\text{INH}}$  can be expressed as the sum of two components reflecting energy losses in charge separation reaction and energy losses in the antenna:  $k^{\text{INH}} = k_1^{\text{INH}} k_d^{\text{INH}} / (k_{-1}^{\text{INH}} + k_d^{\text{INH}}) + k_{\text{el}}^{\text{INH}}$ . The apparent independence of effective  $k^{\text{INH}}$  on the capability of the photoinhibited centers to form a charge-separated state indicates that the contribution of the ratio  $k_1^{\text{INH}} k_d^{\text{INH}} / (k_{-1}^{\text{INH}} + k_d^{\text{INH}})$  is minor. Indeed, if we assume that values of the rate constants characterizing charge separation in the photoinhibited PSII are equal to those in the open PSII centers, i.e.,  $k_1^{\text{INH}} = k_1^{\text{OX}}$ ,  $k_{-1}^{\text{INH}} = k_{-1}^{\text{OX}}$ ,  $k_d^{\text{INH}} = k_d^{\text{OX}}$ , the ratio of  $k_1^{\text{INH}} k_d^{\text{INH}} / (k_{-1}^{\text{INH}} + k_d^{\text{INH}})$  equals  $(99 \text{ ns})^{-1}$ , which is  $>200$  times less than the estimated value of  $k^{\text{INH}}$   $[(0.46 \text{ ns})^{-1}]$ . The above situation might be realized in the photoinhibited centers with protonated  $Q_A^-$  postulated by Vass and co-authors (1992). If we assume that the charge separation and recombination reactions in the photoinhibited PSII occur with rates characteristic of those in closed PSII ( $k_1^{\text{INH}} = k_1^{\text{RED}}$ ,  $k_{-1}^{\text{INH}} = k_{-1}^{\text{RED}}$ ,  $k_d^{\text{INH}} = k_d^{\text{RED}}$ ) the ratio of  $k_1^{\text{INH}} k_d^{\text{INH}} / (k_{-1}^{\text{INH}} + k_d^{\text{INH}})$  turns out to be  $(2.9 \text{ ns})^{-1}$ , which is still 6.3 times less than the value of  $k^{\text{INH}}$ .

If most of the active PSII are in the open state (i.e.,  $\mathbf{o} \gg \mathbf{r}$ ), a fraction of photons collected by the photoinhibited units can be finally trapped by the active open PSII centers because of the high efficiency of exciton exchange between the photoinhibited and active PSII, and because  $k^{\text{OX}} > k^{\text{INH}}$ . In other words, photoinhibition can increase the absorption cross section of open PSII, a conclusion that agrees with measurements of the light-response curves of  $O_2$  evolution in photoinhibited thylakoids (Fig. 3). However, under exposure of isolated thylakoids to the photoinhibitory light, a vast majority of active PSII centers is in the closed state ( $\mathbf{r} \gg \mathbf{o}$ ) because of the absence of an efficient terminal electron acceptor. For this case, the model calculations predict a decrease in the yield of formation of the radical pair  $P680^+Pheo^-$  due to an increase in exciton flow from the closed to the photoinhibited types of PSII units.

The dynamics of PSII photoinhibition in isolated thylakoids fit the first-order kinetics well within a wide range of light intensities (Fig. 1). The exponential decrease in PSII oxygen evolution means that for every active PSII unit the probability to be photoinactivated in unit time is constant throughout the photoinhibitory period and independent of the concentration of photoinhibited PSII units. Values of the rate constant of photoinhibition  $k_{\text{PI}}$  calculated on the basis of the above experiment were directly proportional to the light intensity (inset to Fig. 1), indicating that the quantum efficiency of PSII photoinhibition is constant throughout the wide range of light intensities. We have earlier shown that the above characteristics apply for photoinhibition of intact leaves (Tyystjärvi and Aro, 1996).

Various mechanisms of PSII photoinhibition have been proposed. If the oxygen-evolving side does not function, the photoinhibitory damage to PSII has been suggested to occur via formation of such radicals as  $P680^+$  and/or  $Tyr_Z^+$  (Blubaugh and Cheniae, 1990; Vermaas et al., 1995). In preparations with a fully active oxidizing side of PSII, photoinhibition has been suggested to occur through formation of doubly reduced  $Q_A$  (Vass et al., 1992), through back-recombination of charges  $P680^+Pheo^-$  (or  $S_nQ_A^-$ ) producing triplet P680 and then singlet oxygen (Durrant et al., 1990; Ohad et al., 1994), and by means of electron transfer from  $Q_A^-$  (or  $Q_B^-$ ) to molecular oxygen forming the superoxide anion radical (Kyle, 1987). The distinguishing feature of the mechanisms listed is that all of them presume the reactions of electron transfer or charge separation prior to photoinhibition of oxygen evolution. Therefore, in theory, the yield of photoinhibition should be more or less proportional to the efficiency of formation of the radical pair  $P680^+Pheo^-$ , which was shown to decrease when photoinhibition proceeds (Fig. 8). Consequently, one would expect a noticeable deviation of the photoinhibitory kinetics from a single exponential. Such deviation, however, was not seen.

It might be assumed that a strong quenching process (e.g., energy-dependent quenching, qE), which can develop in thylakoids exposed to a strong light, masks the quenching by the photoinhibited PSII units, thus yielding a nearly exponential decay of PSII activity during the photoinhibition treatment. This, however, was not the case in our study because the photoinhibitory experiments were done with uncoupled thylakoids, in which no energy-dependent quenching was observed and the  $F_M$  values measured in the course of strong illumination were virtually the same as the  $F_M$  values measured from the illuminated thylakoids after dark adaptation of several minutes (data not shown).

The apparent contradiction between the proposed decrease in the yield of formation of the radical pair  $P680^+Pheo^-$  and the single-exponential kinetics of photoinhibition might be a consequence of enhanced generation of harmful oxygen species in thylakoids exposed to a strong light, which may essentially compensate for the protection afforded by the quenching of excitation energy in the photoinhibited centers. An increase in production of singlet oxygen with the decrease in PSII activity in illuminated thylakoids was reported by Hideg et al. (1994). It was suggested that those photoinhibited PSII units that are still capable of charge separation have an increased yield of singlet oxygen generation. Singlet oxygen production can continue even after destruction of P680 due to triplet formation by intersystem crossing in antenna pigments (Mishra et al., 1994). It could be argued that the harmful oxygen species are too reactive to diffuse out of one PSII unit and to do harm to a neighboring (active) PSII unit. However, singlet oxygen produced by illuminated PSII can be detected from its interaction with tetramethylpiperidine (Hideg et al., 1994), indicating that diffusion occurs. It has also been reported that in thylakoid suspension certain protection from photoinhibition can be achieved by adding



bovine albumin (Hideg et al., 1995) or histidine (Mishra et al., 1994), both known to quench singlet oxygen (see, for example, Matheson et al., 1975). Moreover, numerous studies show that addition of singlet-oxygen-generating substances, such as rose bengal or hydrogen peroxide-hypochlorite mixture, results in a similar PSII inactivation and D1 protein fragmentation to that seen during photoinhibition (Mishra et al., 1994; Miyao, 1994). The above data suggest that harmful oxygen species formed by one PSII unit may interact with a nearby second unit, in particular taking into account that PSII units are likely to be organized in the membrane as a connected package.

Another possible explanation for the first-order kinetics of photoinhibition, as well as the direct proportionality between the rate-constant of photoinhibition and light intensity (see inset to Fig. 1) is that photoinhibition requires the absorption of light by pigments that are energetically disconnected from the antenna, i.e., the light-induced damage to PSII occurs independently of the primary photosynthetic reactions. This explanation, suggested earlier by Tyystjärvi (1993) and Sinclair et al. (1996) lacks spectroscopic evidence but is tempting because it does not require diffusion of any active form of oxygen. Apart from the present results, independence of photoinhibition on primary electron transfer reactions can be interpreted from the data of Keren et al. (1997) demonstrating that photoinhibition occurs at the same rate in thylakoids subjected to 30  $\mu\text{mol photons m}^{-2} \text{ s}^{-1}$  whether the light is given in the form of continuous light or in the form of laser pulses separated by 40 s of darkness. In such a system every PSII unit would utilize tens of photons during the 40-s period of continuous illumination, whereas the PSII units subjected to the laser excitation utilized only one photon during the same time interval. More work is needed to elucidate the mechanism of photoinhibition and to understand the first-order kinetics of photoinhibition.

## APPENDIX

List of symbols used throughout the text:

$F_O$ , $F_M$ , and $F_V$	the measured initial, maximal and variable fluorescence, respectively
$\Phi$	total yield of exciton decay
$\Phi_{fl}$	calculated fluorescence yield
$\Phi_p$	calculated yield of $Q_A$ reduction
$\Phi_O$ , $\Phi_M$ , $\Phi_V$	the calculated yields of initial, maximal, and variable fluorescence
$\Phi_V^{\text{max}}$	maximum yield of variable fluorescence
$I$	rate of exciton creation per PSII center
$i$	fraction of photoinhibited PSII units
$k_1$	apparent rate constant for primary charge separation
$k_{-1}$	rate constant of charge recombination
$k_2$	rate constant for charge stabilization (reduction of $Q_A$ )
$k_{el}$	rate constant for energy losses in antenna (including radiative pathway)
$k_{fl}$	rate constant for radiative losses in antenna
$k_d$	rate constant for nonradiative losses of the radical pair

$k_{uu}$	rate constant for exciton transfer between PSII units
$k_{PI}$	rate constant of photoinhibition
$o$	fraction of PSII units in open state ( $Q_A$ oxidized)
$r$	fraction of PSII units in closed state ( $Q_A$ reduced)
$R$	concentration of the PSII radical pairs
$t$	time
$U$	antenna system of PSII unit
$\omega$	relative amount of open PSII [ $\omega = o/(1 - i)$ ]
$z$	concentration of excitons

Superscripts "ACT," "INH," "OX," and "RED" refer to PSII units in active, photoinhibited, open, and closed state, respectively.

A method for obtaining analytical solutions for the fluorescence and photochemistry in a model similar to that one depicted in Fig. 4 was described in detail by Lavergne and Trissl (1995). The following treatment shows the outlines of the calculation. A detailed description can be found in the Internet (<http://www.utu.fi/ml/kasvimb/analytic.html>).

At the first step, the exciton-radical pair model is transformed into a scheme with irreversible decay processes (Fig. 5). The analytical expressions linking the effective rate constants  $k^{\text{INH}}$ ,  $k^{\text{OX}}$  and  $k^{\text{RED}}$  to the rate constants describing the charge separation reactions depicted in Fig. 4 are listed below:

$$k^{\text{INH}} = k_{el}^{\text{INH}} \quad (1a)$$

$$k^{\text{OX}} = L_p + L_d + k_{el}^{\text{ACT}} \quad (1b)$$

$$k^{\text{RED}} = L_b + k_{el}^{\text{ACT}} \quad (1c)$$

where

$$L_p = k_1^{\text{OX}} k_2^{\text{OX}} / (k_{-1}^{\text{OX}} + k_2^{\text{OX}} + k_d^{\text{OX}}) \quad (2a)$$

$$L_d = k_1^{\text{OX}} k_d^{\text{OX}} / (k_{-1}^{\text{OX}} + k_2^{\text{OX}} + k_d^{\text{OX}}) \quad (2b)$$

$$L_b = k_1^{\text{RED}} k_d^{\text{RED}} / (k_{-1}^{\text{RED}} + k_d^{\text{RED}}) \quad (2c)$$

At the next step the irreversible decay scheme is substituted by a random-walk network in which the rate constants are replaced by hopping probabilities  $p_{jl}$  among the three states of PSII. The hopping probabilities are linked to the rate constants as follows:  $p_{jl} = k_{jl} / \sum_{l=1}^3 k_{jl}$ , where  $j = 1, 2, 3$  and  $l = 1, 2, 3$  indicate three states of PSII units ( $U^{\text{INH}}$ ,  $U^{\text{OX}}$ , or  $U^{\text{RED}}$ , respectively) and  $k_{jl}$  indicate the rate constants for corresponding reactions of exciton migration or decay. Denoting by  $P(j, l)$  the total probability that an exciton starting from  $j$ th state will eventually decay from  $l$ th state one can express  $P(j, l)$  through the hopping probabilities  $p_{jl}$  and consequently through the rate constants  $k_{jl}$  as shown in Lavergne and Trissl (1995). The total yields  $\Phi$  of exciton decay from open, closed, and photoinhibited PSII states with regard to initial distributions of excitons are:

$$\Phi^{\text{OX}} = i P(1, 2) + o P(2, 2) + (1 - i - o) P(3, 2) \quad (3a)$$

$$\Phi^{\text{RED}} = i P(1, 3) + o P(2, 3) + (1 - i - o) P(3, 3) \quad (3b)$$

$$\Phi^{\text{INH}} = 1 - \Phi^{\text{OX}} - \Phi^{\text{RED}} \quad (3c)$$

The photochemical yield of  $Q_A$  reduction  $\Phi_p$  and the total yield of fluorescence  $\Phi_{fl}$  can be written as

$$\Phi_p = L_p \Phi^{\text{OX}} / k^{\text{OX}} \quad (4)$$

$$\Phi_{fl} = k_{fl}^{\text{INH}} \Phi^{\text{INH}} / k^{\text{INH}} + k_{fl}^{\text{ACT}} \Phi^{\text{RED}} / k^{\text{RED}} + k_{fl}^{\text{ACT}} \Phi^{\text{OX}} / k^{\text{OX}} \quad (5)$$

Substituting  $\Phi^{\text{OX}}$ ,  $\Phi^{\text{RED}}$ , and  $\Phi^{\text{INH}}$  in Eqs. 4 and 5 by the values calculated in Eqs. 3a–c, then substituting the expressions of  $P(j, l)$  by their values as functions of hopping probabilities  $p_{jl}$  and finally substituting the hopping probabilities by their expressions as functions of the rate constants, results in the following expressions for the yields of fluorescence



$\Phi_n$  and photochemistry  $\Phi_p$ :

$$\Phi_p = \frac{\mathcal{A}\mathbf{o}}{1 + \mathcal{J}\mathbf{o}} \quad (6)$$

$$\Phi_n = \frac{\mathcal{B} + \mathcal{C}\mathbf{o}}{1 + \mathcal{J}\mathbf{o}} \quad (7a)$$

where

$$\mathcal{A} = \frac{L_p(k_{uu}^{\text{INH}} + k_{uu}^{\text{ACT}})}{[k^{\text{OX}} + k_{uu}^{\text{ACT}} + \mathbf{i}(k_{uu}^{\text{INH}} - k_{uu}^{\text{ACT}})]} \times \frac{[k^{\text{RED}} + k_{uu}^{\text{ACT}} + \mathbf{i}(k_{uu}^{\text{INH}} - k_{uu}^{\text{ACT}})]}{[k^{\text{RED}}(k_{uu}^{\text{INH}} + k_{uu}^{\text{INH}}) + \mathbf{i}k_{uu}^{\text{INH}}(k^{\text{INH}} - k^{\text{RED}})]} \quad (8a)$$

$$\mathcal{B} = \frac{k_n^{\text{ACT}}[\mathbf{i}(k^{\text{RED}} - k^{\text{INH}}) + k^{\text{INH}} + k_{uu}^{\text{INH}}]}{[k^{\text{RED}}(k_{uu}^{\text{INH}} + k_{uu}^{\text{INH}}) + \mathbf{i}k_{uu}^{\text{INH}}(k^{\text{INH}} - k^{\text{RED}})]} \quad (8b)$$

$$\mathcal{C} = \frac{k_n^{\text{ACT}}(k^{\text{OX}} - k^{\text{RED}})}{[k^{\text{RED}} + k_{uu}^{\text{ACT}} + \mathbf{i}(k_{uu}^{\text{INH}} - k_{uu}^{\text{ACT}})]} \times \frac{[\mathbf{i}(k_{uu}^{\text{ACT}} - k_{uu}^{\text{INH}}) - k^{\text{INH}} - k_{uu}^{\text{INH}}]}{[k^{\text{RED}}(k_{uu}^{\text{INH}} + k_{uu}^{\text{INH}}) + \mathbf{i}k_{uu}^{\text{INH}}(k^{\text{INH}} - k^{\text{RED}})]} \quad (8c)$$

$$\mathcal{J} = \frac{(k^{\text{OX}} - k^{\text{RED}})}{[k^{\text{OX}} + k_{uu}^{\text{ACT}} + \mathbf{i}(k_{uu}^{\text{INH}} - k_{uu}^{\text{ACT}})]} \times \frac{[k_{uu}^{\text{ACT}}(k_{uu}^{\text{INH}} + k_{uu}^{\text{INH}}) + \mathbf{i}k_{uu}^{\text{INH}}(k_{uu}^{\text{INH}} - k_{uu}^{\text{ACT}})]}{[k^{\text{RED}}(k_{uu}^{\text{INH}} + k_{uu}^{\text{INH}}) + \mathbf{i}k_{uu}^{\text{INH}}(k^{\text{INH}} - k^{\text{RED}})]} \quad (8d)$$

With the definitions  $\Phi_o = \Phi_n(\mathbf{o} = 1 - \mathbf{i})$ ,  $\Phi_M = \Phi_n(\mathbf{o} = 0)$  and  $\Phi_V^{\text{max}} = \Phi_M - \Phi_o$  we can rewrite Eq. 7 as

$$\Phi_o = \frac{\mathcal{B} + \mathcal{C}(1 - \mathbf{i})}{1 + \mathcal{J}(1 - \mathbf{i})} \quad (9)$$

$$\Phi_M = \mathcal{B} \quad (10)$$

$$\Phi_V(\mathbf{o}) = \frac{\Phi_V^{\text{max}}(1 - \mathbf{o} - \mathbf{i})}{1 + \mathcal{J}\mathbf{o}}, \quad (11)$$

where

$$\Phi_V^{\text{max}} = \frac{(\mathcal{B}\mathcal{J} - \mathcal{C})(1 - \mathbf{i})}{1 + \mathcal{J}(1 - \mathbf{i})} \quad (12)$$

An analytical solution for the fluorescence induction kinetics can be deduced, noting that

$$-\frac{d\mathbf{o}}{dt} = \mathbf{I}\Phi_p(\mathbf{o}), \quad (13)$$

where  $\mathbf{I}$  is the rate of exciton creation per reaction center. By integrating Eq. 13 and considering the initial condition  $\mathbf{o} = 1 - \mathbf{i}$  for  $t = 0$ , we obtain

$$t = \frac{\ln \frac{1 - \mathbf{i}}{\mathbf{o}} + \mathcal{J}(1 - \mathbf{i} - \mathbf{o})}{\mathbf{I}\mathcal{A}} \quad (14)$$

By introducing the relative amount of open PSII centers  $\omega = \mathbf{o}/(1 - \mathbf{i})$ , Eqs. 11 and 14 take the following form:

$$\Phi_V(\omega) = \frac{\Phi_V^{\text{max}}(1 - \omega)}{1 + \mathcal{J}(1 - \mathbf{i})\omega}, \quad (15)$$

$$t = \frac{\mathcal{J}(1 - \mathbf{i})(1 - \omega) - \ln \omega}{\mathbf{I}\mathcal{A}} \quad (16)$$

The fluorescence induction kinetics can now be obtained by varying the value of  $\omega$  ( $0 < \omega \leq 1$ ), substituting it into Eqs. 15 and 16 and plotting the calculated  $\Phi_n$  against  $t$ . As could be seen from these equations only three phenomenological parameters ( $\Phi_V^{\text{max}}$ ,  $\mathcal{J}_\alpha(1 - \mathbf{i}_\alpha)$ , and  $\mathbf{I}_\alpha\mathcal{A}_\alpha$ ) determine the variable part of fluorescence induction in a system of PSII $_\alpha$  (active plus photoinhibited) centers, whereas the forth parameter, equal to  $\mathcal{B}_\alpha + \mathcal{C}_\alpha(1 - \mathbf{i}_\alpha)$ , is required for the calculation of  $\Phi_{o\alpha}$ .

For the PSII $_\beta$  centers with no exciton exchange between the PSII units,  $k_{uu}^{\text{ACT}} = 0$ . It is reasonable to assume also that  $k_{uu}^{\text{INH}} = 0$  for PSII $_\beta$ . In this case, as can be deduced from Eq. 8d,  $\mathcal{J} = 0$  and, considering Eqs. 15 and 16, one obtains an exponential form of the variable component of fluorescence induction kinetics, controlled by two phenomenological parameters  $\mathbf{I}_\beta\mathcal{A}_\beta$  and  $\Phi_V^{\text{max}}$ :

$$\Phi_{V\beta}(t) = \Phi_{V\beta}^{\text{max}} \left\{ 1 - \exp\left(-\frac{t}{\mathbf{I}_\beta\mathcal{A}_\beta}\right) \right\} \quad (17)$$

To calculate the effect of the photoinhibited PSII on the yield of the radical pair formation in thylakoids exposed to a strong light we considered the reaction scheme shown in Fig. 4, which was simplified by assuming that all the PSII centers are either in the active closed or in the photoinhibited state ( $\mathbf{i} + \mathbf{r} = 1$ ). The behavior of such a system can be described by the following set of first-order differential equations:

$$dz^{\text{INH}}/dt = \mathbf{I}\mathbf{i} + k_{uu}^{\text{INH}}\mathbf{i}z^{\text{RED}} - k_{\text{el}}^{\text{INH}}z^{\text{INH}} - k_{uu}^{\text{INH}}\mathbf{r}z^{\text{INH}} \quad (18a)$$

$$dz^{\text{RED}}/dt = \mathbf{I}\mathbf{r} + k_{uu}^{\text{INH}}\mathbf{r}z^{\text{INH}} + k_{-1}\mathbf{R} - k_{uu}^{\text{INH}}\mathbf{i}z^{\text{RED}} - k_{\text{el}}^{\text{RED}}z^{\text{RED}} - k_{\text{d}}^{\text{RED}}\mathbf{R} \quad (18b)$$

$$d\mathbf{R}/dt = k_1z^{\text{RED}} - k_{-1}\mathbf{R} - k_{\text{d}}^{\text{RED}}\mathbf{R} \quad (18c)$$

where  $z^{\text{INH}}$  and  $z^{\text{RED}}$  indicate concentrations of excitons in photoinhibited or reduced centers, respectively;  $\mathbf{I}$  is rate of exciton creation (per PSII) and  $\mathbf{R}$  is the concentration of the radical pair.

Under the steady-state illumination  $z^{\text{INH}}$ ,  $z^{\text{RED}}$ , and  $\mathbf{R}$  are constant and therefore the set of differential Eqs. 18a–c can be transformed into a system of linear equations:

$$\mathbf{I}\mathbf{i} + k_{uu}^{\text{INH}}\mathbf{i}z^{\text{RED}} - k_{\text{el}}^{\text{INH}}z^{\text{INH}} - k_{uu}^{\text{INH}}\mathbf{r}z^{\text{INH}} = 0 \quad (19a)$$

$$\mathbf{I}\mathbf{r} + k_{uu}^{\text{INH}}\mathbf{r}z^{\text{INH}} + k_{-1}\mathbf{R} - k_{uu}^{\text{INH}}\mathbf{i}z^{\text{RED}} - k_1z^{\text{RED}} - k_{\text{el}}^{\text{RED}}z^{\text{RED}} = 0 \quad (19b)$$

$$k_1z^{\text{RED}} - k_{-1}\mathbf{R} - k_{\text{d}}^{\text{RED}}\mathbf{R} = 0 \quad (19c)$$

By solving the system one can express  $\mathbf{R}$  as

$$\mathbf{R} = \mathbf{I}k_1(1 - \mathbf{i})(k_{\text{el}}^{\text{INH}} + k_{uu}^{\text{INH}})/\mathcal{D} \quad (20a)$$

where

$$\mathcal{D} = k_{uu}^{\text{INH}}k_{\text{el}}^{\text{INH}}\mathbf{i}(k_{-1} + k_{\text{d}}^{\text{RED}}) + [k_{\text{el}}^{\text{INH}} + k_{uu}^{\text{INH}}(1 - \mathbf{i})](k_{\text{el}}^{\text{RED}}k_{-1} + k_1k_{\text{d}}^{\text{RED}} + k_{\text{el}}^{\text{RED}}k_{\text{d}}^{\text{RED}}) \quad (20b)$$

This work was supported by the Academy of Finland. DVV was supported by a fellowship from the Centre for International Mobility (CIMO).

## REFERENCES

- Anderson, J. M., and E.-M. Aro. 1994. Grana stacking and protection of Photosystem II in thylakoid membranes of higher plant leaves under sustained high irradiance: an hypothesis. *Photosynth. Res.* 41:315–326.
- Aro, E.-M., I. Virgin, and B. Andersson. 1993. Photoinhibition of Photosystem II. Inactivation, protein damage and turnover. *Biochim. Biophys. Acta.* 1143:113–134.
- Blubaugh, D. J., and G. M. Cheniae. 1990. Kinetics of photoinhibition in hydroxylamine-extracted photosystem II membranes. *Biochemistry.* 29: 5109–5118.
- Chow, W. S. 1994. Photoprotection and photoinhibition damage. In *Advances in Molecular and Cell Biology*. Vol. 10. J. Barber, editor. JAI Press Inc., Stamford, CT. 151–196.
- Dau, H. 1994. Molecular mechanisms and quantitative models of variable Photosystem II fluorescence. *Photochem. Photobiol.* 60:1–23.
- Durrant, J. R., L. B. Giorgi, J. Barber, D. R. Klug, and G. Porter. 1990. Characterisation of triplet states in isolated Photosystem II reaction centres: oxygen quenching as a mechanism for photodamage. *Biochim. Biophys. Acta.* 1017:167–175.
- Giersch, C., and H. Krause. 1991. A simple model relating photoinhibitory fluorescence quenching in chloroplasts to a population of altered Photosystem II reaction centres. *Photosynth. Res.* 30:115–121.
- Guenther, J. E., J. A. Nemson, and A. Melis. 1990. Development of Photosystem II in dark-grown *Chlamydomonas reinhardtii*. A light-dependent conversion of PSII<sub>B</sub>, Q<sub>B</sub>-nonreducing centers to the PSII<sub>ox</sub>, Q<sub>B</sub>-reducing form. *Photosynth. Res.* 24:35–46.
- Hideg, É., C. Spetea, and I. Vass. 1994. Singlet oxygen production in thylakoid membranes during photoinhibition as detected by EPR spectroscopy. *Photosynth. Res.* 39:191–199.
- Hideg, É., C. Spetea, and I. Vass. 1995. Superoxide radicals are not the main promoters of acceptor-side-induced photoinhibitory damage in spinach thylakoids. *Photosynth. Res.* 46:399–407.
- Keren, N., A. Berg, P. J. M. van Kam, H. Levanson, and I. Ohad. 1997. Mechanism of photosystem II photoinactivation and D1 protein degradation at low light: the role of back electron flow. *Proc. Natl. Acad. Sci. USA.* 94:1579–1584.
- Krause, G. H. 1994. The role of oxygen in photoinhibition of photosynthesis. In *Causes of Photooxidative Stress and Amelioration of Defense Systems in Plants*. C. H. Foyer and P. M. Mullineaux, editors. CRC Press, Boca Raton, FL. 43–76.
- Krause, G. H., and E. Weis. 1991. Chlorophyll fluorescence and photosynthesis: the basics. *Annu. Rev. Plant Physiol. Plant Mol. Biol.* 42:313–349.
- Kyle, D. J. 1987. The biochemical basis for photoinhibition of Photosystem II. In *Topics in Photosynthesis: Photoinhibition*. Vol. 9. D. J. Kyle, C. B. Osmond, and C. J. Arntzen, editors. Elsevier, Amsterdam. 197–227.
- Lavergne, J., and H.-W. Trissl. 1995. Theory of fluorescence induction in photosystem II: derivation of analytical expressions in a model including exciton-radical-pair equilibrium and restricted energy transfer between photosynthetic units. *Biophys. J.* 68:2474–2492.
- Leibl, W., J. Berton, J. Deprez, and H.-W. Trissl. 1989. Photoelectric study on the kinetics of trapping and charge stabilization in oriented PSII membranes. *Photosynth. Res.* 22:257–275.
- Matheson, I. B. C., R. D. Etheridge, N. R. Kratoch, and J. Lee. 1975. The quenching of singlet oxygen by amino acids and proteins. *Photochem. Photobiol.* 21:165–171.
- Melis, A., and P. H. Homann. 1976. Heterogeneity of the photochemical centres in system II of chloroplasts. *Photochem. Photobiol.* 23:243–350.
- Mishra, N. P., C. Francke, H. J. van Gorkom, and D. F. Ghanotakis. 1994. Destructive role of singlet oxygen during aerobic illumination of the photosystem II core complex. *Biochim. Biophys. Acta.* 1186:81–90.
- Miyao, M. 1994. Involvement of active oxygen species in degradation of the D1 protein under strong illumination in isolated subcomplexes of photosystem II. *Biochemistry.* 33:9722–9730.
- Ohad, I., N. Keren, H. Zer, H. Gong, T. S. Mor, A. Gal, S. Tal, and Y. Domovich. 1994. Light-induced degradation of the Photosystem II reaction centre D1 protein *in vivo*: an integrated approach. In *Photoinhibition of Photosynthesis: from Molecular Mechanisms to the Field*. N. R. Baker and J. R. Bowyer, editors. BIOS Scientific Publishers, Oxford. 161–178.
- Öquist, G., W. S. Chow, and J. M. Anderson. 1992. Photoinhibition of photosynthesis represents a mechanism for the long-term regulation of photosystem II. *Planta.* 186:450–460.
- Porra, R. J., W. A. Thompson, and P. E. Kriedemann. 1989. Determination of accurate extinction coefficients and simultaneous equations for assaying chlorophylls a and b extracted with four different solvents: verification of the concentration of chlorophyll standards by atomic absorption spectroscopy. *Biochim. Biophys. Acta.* 975:384–394.
- Powles, S. B., and O. Björkman. 1982. Photoinhibition of photosynthesis: effect on chlorophyll fluorescence at 77K in intact leaves and in chloroplast membranes of *Nerum oleander*. *Planta.* 156:97–107.
- Prasil, O., N. Adir, and I. Ohad. 1992. Dynamics of photosystem II. Mechanism of photoinhibition and recovery processes. In *Topics in Photosynthesis*. Vol. 11. J. Barber, editor. Elsevier, Amsterdam. 293–348.
- Renger, G., H.-J. Eckert, A. Bergmann, J. Bernarding, B. Liu, A. Napiwotzki, F. Reifarth, and H. G. Eichler. 1995. Fluorescence and spectroscopic studies of exciton trapping and electron transfer in Photosystem II of higher plants. *Aust. J. Plant Physiol.* 22:167–181.
- Rintamäki, E., R. Salo, and E.-M. Aro. 1994. Rapid turnover of the D1 reaction-centre protein of photosystem II as a protection mechanism against photoinhibition in moss *Ceratodon purpureus* (Hedw.) Brid. *Planta.* 193:520–529.
- Roelofs, T. A., C.-H. Lee, and A. R. Holzwarth. 1992. Global target analysis of picosecond chlorophyll fluorescence kinetics from pea chloroplasts: a new approach to the characterization of the primary processes in photosystem II alpha- and beta-units. *Biophys. J.* 61: 1147–1163.
- Satoh, K., M. Ohhashi, Y. Kashino, and H. Koike. 1995. Mechanism of electron flow through the Q<sub>B</sub>-site in photosystem II. I. Kinetics of the reduction of electron acceptors at the Q<sub>B</sub> and plastoquinone sites in photosystem II particles from the cyanobacterium *Synechococcus vulcanus*. *Plant Cell Physiol.* 36:597–605.
- Schatz, G. H., H. Brock, and A. R. Holzwarth. 1988. A kinetic and energetic model for the primary processes in photosystem II. *Biophys. J.* 54:397–405.
- Sinclair, J., Y.-I. Park, W. S. Chow, and J. M. Anderson. 1996. Target theory and the photoinactivation of Photosystem II. *Photosynth. Res.* 50:33–40.
- Styring, S., I. Virgin, A. Ehrenberg, and B. Andersson. 1990. Strong light photoinhibition of electron transport in Photosystem II. Impairment of the function of the first quinone acceptor, Q<sub>A</sub>. *Biochim. Biophys. Acta.* 1015:269–278.
- Trissl, H.-W., and J. Lavergne. 1995. Fluorescence induction from Photosystem II: analytical equations for the yields of photochemistry and fluorescence derived from analysis of a model including exciton-radical pair equilibrium and restricted energy transfer between units. *Aust. J. Plant Physiol.* 22:183–193.
- Tyystjärvi, E. 1993. Photoinhibition: struggle between damage and repair of photosystem II. Doctoral thesis, University of Turku.
- Tyystjärvi, E., and E.-M. Aro. 1996. The rate-constant of photoinhibition, measured in lincomycin-treated leaves, is directly proportional to light intensity. *Proc. Natl. Acad. Sci. USA.* 93:2213–2218.
- Tyystjärvi, E., R. Kettunen, and E.-M. Aro. 1994. The rate-constant of photoinhibition *in vitro* is independent of the antenna size of Photosystem II but depends on temperature. *Biochim. Biophys. Acta.* 1186: 177–185.
- Vass, I., S. Styring, T. Hundal, A. Koivuniemi, E.-M. Aro, and B. Andersson. 1992. Reversible and irreversible intermediates during photoinhibition of Photosystem 2. Stable reduced Q<sub>A</sub> species promote chlorophyll triplet formation. *Proc. Natl. Acad. Sci. USA.* 89:1408–1412.
- Vermaas, W., C. Madsen, Yu. Jiujiang, J. Visser, J. Metz, P. Nixon, and B. Diner. 1995. Turnover of the D1 protein and of Photosystem II in a *Synechocystis* 6803 mutant lacking Tyr<sub>Z</sub>. *Photosynth. Res.* 45:99–104.